Acta Crystallographica Section D
Biological Crystallography
ISSN 0907-4449

Studies on a Tyr residue critical for the binding of coenzyme and substrate in mouse 3(17)α-hydroxysteroid dehydrogenase (AKR1C21): structure of the Y224D mutant enzyme

Urmi Dhagat,[a]‡ Satoshi Endo,[b]‡ Hiroaki Mamiya,[b] Akira Hara[b] and Ossama El-Kabbani[a]*

[a]Medicinal Chemistry and Drug Action, Monash Institute of Pharmaceutical Sciences, Monash University, Parkville, Victoria 3052, Australia, and [b]Laboratory of Biochemistry, Gifu Pharmaceutical University, Mitahora-higashi, Gifu 502-8585, Japan

‡ These authors contributed equally to the work and share first authorship.

Correspondence e-mail: ossama.el-kabbani@vcp.monash.edu.au

Received 25 May 2009
Accepted 29 November 2009

PDB Reference: Y224D mutant AKR1C21, 3fjn.

Mouse 3(17)α-hydroxysteroid dehydrogenase (AKR1C21) is the only aldo–keto reductase that catalyzes the stereospecific reduction of 3- and 17-ketosteroids to the corresponding 3(17)α-hydroxysteroids. The Y224D mutation of AKR1C21 reduced the K_m value for NADP(H) by up to 80-fold and completely reversed the 17α stereospecificity of the enzyme. The crystal structure of the Y224D mutant at 2.3 Å resolution revealed that the mutation resulted in a change in the conformation of the flexible loop B, including the V-shaped groove, which is a unique feature of the active-site architecture of wild-type AKR1C21 and is formed by the side chains of Tyr224 and Trp227. Furthermore, mutations (Y224F and Q222N) of residues involved in forming the safety belt for binding of the coenzyme showed similar alterations in kinetic constants for 3α-hydroxy/3-ketosteroids and 17-hydroxy/ketosteroids compared with the wild type.

1. Introduction

The aldo–keto reductase (AKR) superfamily comprises a group of structurally related proteins that metabolize a wide range of substrates including steroids, polycyclic aromatic hydrocarbons, aromatic and aliphatic aldehydes, monosaccharides, prostaglandins and isoflavonoids (Penning *et al.*, 1996; Hyndman *et al.*, 2003). These enzymes share a common TIM-barrel structural motif consisting of an eight-stranded parallel β-sheet core surrounded by eight α-helices running antiparallel to the sheet. The C-terminal ends of the β-strands are connected to the amino-termini of the α-helices by loops of varying lengths (Jez & Penning, 2001; Penning *et al.*, 2004). There are three loops at the C-terminal end of the barrel, namely loop A (residues 118–143), loop B (residues 217–238) and loop C (residues 299–323; numbering is based on the AKR1C21 sequence). Sequence-alignment comparisons of various AKRs revealed that the amino-acid sequences forming the barrel are well conserved compared with those forming the loop regions. The conserved regions seemingly maintain the architecture of the barrel, while residues belonging to the loop regions discriminate between several structurally related substrates and act as specificity determinants (Matsuura *et al.*, 1998; Janecek, 1996; Jez *et al.*, 1997). The reactions catalyzed by AKR enzymes follow an ordered bi-bi mechanism in which the coenzyme binds first and leaves last. Upon coenzyme binding, a portion of loop B undergoes a conformational change that locks the coenzyme in position for catalysis. All AKRs exhibit strong affinity for the coenzyme molecule and the mode of coenzyme binding is conserved across all family members (Borhani *et al.*, 1992; Penning, 1999).

Mouse 3(17)α-hydroxysteroid dehydrogenase (AKR1C21) is a new member of the AKR superfamily (Ishikura *et al.*, 2004; Nakagawa *et al.*, 1989). The enzyme has generated interest owing to its unique ability to stereospecifically reduce ketosteroids at the C17 position to produce 17α-hydroxysteroids. It is the only enzyme known to catalyze the conversion of 4-androstene-3,17-dione to epitestosterone (epi-T), a 17α-epimer of testosterone which has been associated with the development of breast and prostate cancers (Bellemare *et al.*, 2005; Courter *et al.*, 2008). We have reported the inhibition of AKR1C21 by aldose-reductase inhibitors such as tolrestat and quercetin (Dhagat *et al.*, 2008) and more recently determined the crystal structure of the first ternary complex with an inhibitor bound (Dhagat *et al.*, 2009). Knowledge of the binding mode of the inhibitor hexestrol and the residues (Leu25, Lys31, Tyr55, His117, Tyr118, Tyr224 and Trp227) involved in lining the inhibitor-binding site may lead to the development of new compounds with improved potency towards the 17α reductase activity of AKR1C21, a feature that may be useful in the development of new anticancer agents.

Attempts to explain the unique ability of AKR1C21 to reduce ketosteroids to the respective 17α-hydroxysteroids have recently been carried out using crystallographic and molecular-modelling methods (Faucher *et al.*, 2007; Dhagat *et al.*, 2007). From these studies, Tyr224 was identified as an important residue that forms a hydrophobic V-shaped groove together with Trp227 that is unique to the active site of this enzyme. Here, we investigated the role of Tyr224 in determining the stereospecificity of AKR1C21 by preparing the mutants Y224D and Y224F (as well as Q222N) and examined their effects on substrate and coenzyme binding. Interestingly, the Y224D mutation of AKR1C21 reduced the affinity for coenzyme binding and completely reversed the 17α stereospecificity of the enzyme. Furthermore, the crystal structure of the Y224D mutant was determined and together with the mutagenesis results demonstrates the critical role of Tyr224 in the stereospecificity and coenzyme binding of the enzyme.

2. Materials and methods

2.1. Site-directed mutagenesis and purification of recombinant enzymes

Mutagenesis of Q222N, Y224F and Y224D was performed using the QuikChange site-directed mutagenesis kit (Stratagene) with the pkk223-3 expression plasmid harbouring the cDNA for AKR1C21 as the template according to the protocol described by the manufacturer (Ishikura *et al.*, 2004). The primer pairs used for the mutagenesis were composed of sense and antisense oligonucleotides to alter the codons of AKR1C21 cDNA. The coding regions of the cDNAs in the expression plasmids were sequenced using a Beckman CEQ2000XL DNA sequencer in order to confirm the presence of the desired mutation and to ensure that no other mutations had occurred. The recombinant wild-type (WT) and mutant AKR1C21s were expressed in *Escherichia coli* JM109 and purified to homogeneity as described previously (Ishikura *et al.*, 2004). Purity was confirmed by SDS–PAGE and the protein concentration was determined using a bicinchoninic acid protein-assay reagent kit (Pierce, Rockford, Illinois, USA) with bovine serum albumin as the standard.

2.2. Assay of enzyme activity

The dehydrogenase and reductase activities were assayed by measuring the rate of change of NADPH fluorescence (at 455 nm with an excitation wavelength of 340 nm) and absorbance (at 340 nm), respectively, at 298 K. The reaction mixture for the dehydrogenase-activity assay consisted of 0.1 *M* potassium phosphate buffer pH 7.0 and 0.25 m*M* $NADP^+$, hydroxysteroid and enzyme in a total volume of 2.0 ml. NADPH (0.1 m*M*) was used as the coenzyme in the assay of reductase activity for ketosteroids. The apparent K_m and k_{cat} values for substrates and coenzymes were determined by fitting the initial velocities to the Michaelis–Menten equation and are expressed as the mean $\pm$ standard deviation of at least three determinations. Steroids were obtained from Steraloids (Newport, Rhode Island, USA) and Sigma–Aldrich Chemicals.

2.3. Product identification

Identification of the products of the reduction of 4-androstene-3,17-dione was carried out as described previously (Dhagat *et al.*, 2009). Briefly, the substrate (10 μM) was incubated for 30 min at 310 K in 0.1 *M* potassium phosphate pH 7.0 containing 0.25 m*M* NADPH and enzyme. The substrate and products were extracted into ethyl acetate, analyzed by thin-layer chromatography (TLC) and visualized by spraying with ethanol/H_2SO_4 [1:1(*v*:*v*)] solution and heating at 373 K for 1 h. The colour densities of the steroids were measured by a Fujifilm BAS-3000 system using the program *Multi Gauge* v.3.0.

2.4. Crystallization and data collection

Purified Y224D mutant (20 mg ml^{-1}) was mixed with a threefold molar excess of the coenzyme NADPH. Crystallization of the enzyme–coenzyme complex was attempted using Hampton Research Crystal Screens 1 and 2. Crystallization was set up in Linbro plates using the hanging-drop vapour-diffusion method, in which the droplets were placed on siliconized cover slips and allowed to equilibrate against 1 ml reservoir solution at 295 K. Initially, crystals were obtained from Hampton Research Crystal Screen 1 condition No. 18 (0.1 *M* sodium cacodylate pH 6.5, 0.2 *M* magnesium acetate, 20% PEG 8000). This condition was then optimized by varying the concentrations of magnesium acetate and PEG 8000. From droplets in which equal volumes (2 µl) of the protein sample and the final crystallization buffer from the reservoir (0.1 *M* sodium cacodylate, 0.3 *M* magnesium acetate, 20% PEG 8000) were mixed, plate-shaped crystals appeared within one week and diffracted to a resolution of 2.3 Å. X-ray diffraction images were recorded from a single crystal soaked in a cryoprotectant solution (20% ethylene glycol added to the crystallization buffer) and flash-cooled to 100 K using a MAR-345

image plate mounted on a Rigaku RU-300 rotating-anode generator operating at 50 kV and 90 mA (λ = 1.54179 Å). The data were processed and scaled using *HKL*-2000 and *SCALEPACK* (Otwinowski & Minor, 1997). The structure was determined by the molecular-replacement method with the program *MOLREP* from the *CCP*4 suite (Collaborative Computational Project, Number 4, 1994; Storoni *et al.*, 2004) using the atomic coordinates of the WT AKR1C21 binary complex (Dhagat *et al.*, 2007; PDB code 2p5n) as the search model. Following an initial round of rigid-body refinement, the structure was subjected to several rounds of noncrystallographic symmetry-restrained refinement and manual fitting of the amino-acid side chains into $2F_o - F_c$ and $F_o - F_c$ electron-density maps. The structure was built and visualized in *Coot* and refined using *REFMAC*5 (Murshudov *et al.*, 1997; Emsley & Cowtan, 2004). In the final stages of the refinement water molecules were added to the model and the structure was validated using *PROCHECK* (Laskowski *et al.*, 1993).

3. Results and discussion

The key residues that interact with steroid substrates have been identified previously based on the crystal structure of AKR1C21 in complex with epi-T and molecular-modelling studies (Faucher *et al.*, 2007; Dhagat *et al.*, 2007). In addition to the catalytic residues Tyr55 and His117, key residues included Lys31, Gly225 and Gly226, which form hydrogen bonds to the substrates, and Tyr224, which forms a V-shaped groove together with the indole ring of Trp227. The V-shaped groove serves as a docking region for the methyl groups of the steroids and plays an important role in stabilizing the substrates in the active site by making van der Waals contacts with hydrophobic parts of the substrate molecule. The role of Gly225 and Gly226 in dictating the stereospecificity of AKR1C21 has recently been examined by crystallographic, mutagenic and kinetic analyses (Dhagat *et al.*, 2009). Mutation of the two residues to prolines led to a considerable reduction in the 17α-hydroxysteroid dehydrogenase (HSD) activity of the enzyme, but did not abolish it. Trp227 is highly conserved in other members of the AKR superfamily and its mutation severely impairs steroid binding (Jez *et al.*, 1996). Tyr224, on the other hand, is not well conserved in AKR-family members and its role in steroid binding and dictating the stereospecificity of the WT enzyme has not been investigated. Owing to the unique orientation of Tyr224, which forms a V-shaped groove in the active site of the WT enzyme, and its presence within the coenzyme-binding site, it was proposed that Tyr224 plays a crucial role in the binding of both substrate and coenzyme.

In the crystal structure of the ternary complex of WT AKR1C21 with epi-T, the side-chain hydroxyl of Tyr224 interacts with the side-chain amide of Gln222 and the pyrophosphate moiety of the coenzyme (Fig. 1). This hydrogen-bonding network is likely to contribute to the unique orientation of the side chain of Tyr224 that forms the V-shaped groove in the active site. The side-chain amide of Gln222 also forms an important hydrogen bond to the main-chain carbonyl of Ala24, which has been proposed to form a safety belt that stabilizes coenzyme binding (Faucher *et al.*, 2006). These observations suggest that the interaction between Tyr224, Gln222 and the pyrophosphate moiety of the coenzyme is crucial for proper functioning of the enzyme. To determine the role of Tyr224 in substrate and coenzyme binding and in dictating the stereospecificity of the enzyme, two different mutants of Tyr224 were prepared. Firstly, the Y224F mutant was prepared to remove the hydrogen-bonding interactions of the hydroxyl group of Tyr224 with the side-chain amide of Gln222 and the pyrophosphate moiety of the coenzyme. Secondly, the Y224D mutant was prepared to study the effect of replacing a bulky phenol ring with an acidic side chain on the binding of substrates and coenzymes. Gln222 was

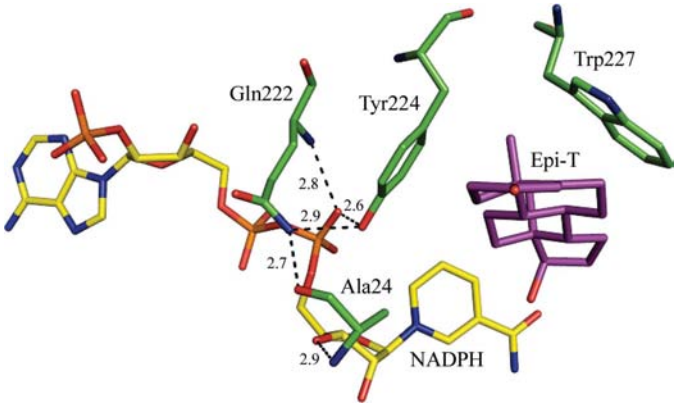

Figure 1
Hydrogen-bonding interactions between Tyr224, Gln222 and the pyrophosphate moiety of NADPH in the active site of the WT AKR1C21–epi-T ternary complex (PDB code 2ipf; Faucher *et al.*, 2007).

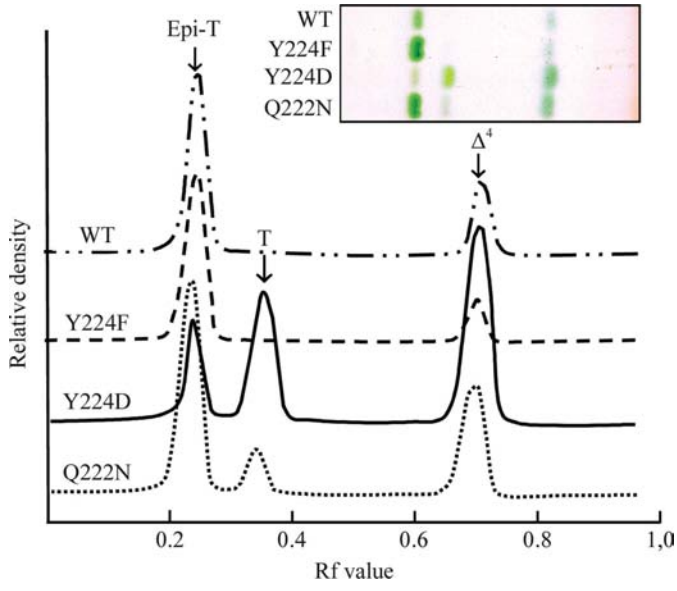

Figure 2
TLC analysis of the products, epi-T and testosterone (T), of the reduction of 4-androstene-3,17-dione (Δ^4) by WT, Y224F, Y224D and Q222N AKR1C21. The density of the coloured steroids on the TLC chromatogram (inset) was measured. The peaks for the substrate and products were identical to the respective authentic standards (not shown).

Table 1
Alterations of kinetic constants for 3α-hydroxy/3-ketosteroids in the mutations.

		Y224F		Y224D		Q222N	
Substrate	WT†	Value	Ratio‡	Value	Ratio‡	Value	Ratio‡
3α-Hydroxysteroids							
5β-Pregnane-3α,20α-diol							
K_m (μM)	0.6	3.2 ± 0.3	5	18 ± 1	30	3.8 ± 0.3	6
k_{cat} (min^{-1})	13	24 ± 1	2	0.22 ± 0.02	0.02	15 ± 2	1
k_{cat}/K_m (min^{-1} μM^{-1})	22	7.5	0.3	0.1	0.05	3.9	0.2
Lithocholic acid							
K_m (μM)	0.1	0.2 ± 0.03	2	6.7 ± 0.2	67	0.6 ± 0.1	6
k_{cat} (min^{-1})	2.8	4.9 ± 0.1	2	0.44 ± 0.03	0.2	6.3 ± 0.3	2
k_{cat}/K_m (min^{-1} μM^{-1})	28	24	1	0.07	0.003	11	0.4
3-Ketosteroids							
5β-Pregnan-20α-ol-3-one							
K_m (μM)	0.2	0.6 ± 0.1	4	15 ± 2	75	0.7 ± 0.1	4
k_{cat} (min^{-1})	23	290 ± 11	13	75 ± 5	3	170 ± 5	7
k_{cat}/K_m (min^{-1} μM^{-1})	120	480	4	5.0	0.04	240	2
5β-Pregnane-3,20-dione							
K_m (μM)	0.6	0.5 ± 0.1	0.8	5.9 ± 0.4	10	0.4 ± 0.1	0.7
k_{cat} (min^{-1})	24	240 ± 30	10	21 ± 2	0.9	290 ± 20	12
k_{cat}/K_m (min^{-1} μM^{-1})	40	480	12	3.6	0.09	720	18

† Taken from Ishikura *et al.* (2004). ‡ Ratio of the mutant enzyme to the WT enzyme.

Table 2
Alteration of kinetic constants for 17-hydroxy/ketosteroids in the mutations.

		Y224F		Y224D		Q222N	
Substrate	WT†	Value	Ratio‡	Value	Ratio‡	Value	Ratio‡
17α-Hydroxysteroids							
Epi-T							
K_m (μM)	0.6	14 ± 1	23		—	20 ± 2	33
k_{cat} (min^{-1})	18	34 ± 2	2	na§	—	14 ± 2	0.8
k_{cat}/K_m (min^{-1} μM^{-1})	30	2.4	0.08		—	0.70	0.02
5α-Androstan-17α-ol-3-one							
K_m (μM)	0.4	5.4 ± 0.1	14		—	14 ± 1	35
k_{cat} (min^{-1})	10	52 ± 5	5	na§	—	17 ± 2	2
k_{cat}/K_m (min^{-1} μM^{-1})	25	9.6	0.4		—	1.2	0.05
17β-Hydroxysteroids							
5α-Androstan-17β-ol-3-one							
K_m (μM)		4.7 ± 0.1	—	96 ± 7	—	82 ± 8	—
k_{cat} (min^{-1})	na§	0.16 ± 0.01	—	0.15 ± 0.02	—	2.2 ± 0.1	—
k_{cat}/K_m (min^{-1} μM^{-1})		0.03	—	0.002	—	0.027	—
5-Androstene-3β,17β-diol							
K_m (μM)		13 ± 2	—	35 ± 1	—	100	—
k_{cat} (min^{-1})	na§	0.13 ± 0.02	—	0.10 ± 0.02	—	3.9 ± 0.3	—
k_{cat}/K_m (min^{-1} μM^{-1})		0.01	—	0.003	—	0.039	—
17-Ketosteroids							
4-Androstene-3,17-dione							
K_m (μM)	0.2	1.5 ± 0.1	8	7.8 ± 0.2	39	5.9 ± 0.2	30
k_{cat} (min^{-1})	10	19 ± 2	2	1.3 ± 0.2	0.1	37 ± 2	4
k_{cat}/K_m (min^{-1} μM^{-1})	50	13	0.3	0.2	0.004	6.3	0.1
5α-Androstan-3α-ol-17-one							
K_m (μM)	0.6	1.8 ± 0.2	3	15 ± 1	25	3.4 ± 0.1	6
k_{cat} (min^{-1})	4.4	7.6 ± 0.8	2	1.3 ± 0.2	0.3	14 ± 2	3
k_{cat}/K_m (min^{-1} μM^{-1})	7.3	4.2	0.6	0.09	0.01	4.1	0.6

† Taken from Ishikura *et al.* (2004) and Dhagat *et al.* (2009). ‡ Ratio of the mutant enzyme to the WT enzyme. § na, no activity was detected.

also mutated to asparagine, which can no longer form the safety belt by hydrogen bonding to Ala24.

Various hydroxysteroids were tested as substrates for the three mutants Y224F, Y224D and Q222N in order to study the effect of the mutations on the stereospecificity of the enzyme. Overall, the mutants oxidized 3α-hydroxysteroids, including lithocholic acid (Table 1), and did not exhibit dehydrogenase activity towards 3β-hydroxysteroids (5α/β-pregnan-3β-ol-20-ones, 5α/β-androstan-3β-ol-17-ones and 5-androsten-3β-ol-17-one) and 20-hydroxysteroids (5α/β-pregnan-20α/β-ol-3-ones and 20α/β-hydroxyprogesterones). However, while mutagenesis did not affect the stereospecific oxidation of the C-3 hydroxyl group of the steroid substrate, it resulted in a change from the strict 17α stereospecificity of AKR1C21 (Table 2). The Y224F and Q222N mutants oxidized 17β-hydroxysteroids (5α-androstan-17β-ol-3-one and 5-androstene-3β,17β-diol) as well as the proper 17α-hydroxysteroid substrates (epi-T and 5α-androstan-17α-ol-3-one). In addition, the Y224D mutant only exhibited dehydrogenase activity on 17β-hydroxysteroids. This change in the stereospecificity on mutation was also observed in the reverse reaction, the reduction of 4-androstene-3,17-dione by Y224D and Q222N mutants, in which the 17β-hydroxy metabolite testosterone was detected by TLC analysis (Fig. 2).

To assess the kinetic effect of the mutagenesis, the kinetic constants for representative 3α- and 17-hydroxy/ketosteroids are compared in more detail for WT AKR1C21 and the three mutants. In the oxidoreduction of 3α-hydroxy/ketosteroids (Table 1), the two mutations Y224F and Q222N showed almost similar small alterations in kinetic constants for the substrates, except that the k_{cat} values for 5β-pregnane-3,20-dione were increased by about tenfold compared with that of the WT enzyme. In contrast, the Y224D mutation resulted in a large impairment of the kinetic constants for all of the substrates, with >10-fold increases in the K_m values and >20-fold decreases in the k_{cat}/K_m values. In the oxidation of 17-hydroxysteroids (Table 2), the Y224F and Q222N mutations significantly increased the K_m values for 17α-hydroxysteroids, resulting in a decrease in the catalytic efficiencies (k_{cat}/K_m). The 17β-HSD activities of the two mutants were low, as evident from the much lower k_{cat} and k_{cat}/K_m values for 5α-androstan-17β-ol-3-one than for its 17α-isomer 5α-androstan-17α-ol-3-one. The most significant change caused by the Y224D mutation was the disappearance of 17α-HSD activity and the appearance of 17β-HSD activity, although the k_{cat}/K_m values for 17β-hydroxysteroids were lower than those of the Y224F mutant. The Y224D mutant showed larger kinetic

Table 3
Alterations of kinetic constants for coenzymes in the mutations.

	NADP$^+$†		NADPH‡	
Enzyme	K_m (μ*M*)	k_{cat} (min^{-1})	K_m (μ*M*)	k_{cat} (min^{-1})
WT	0.5 ± 0.1	3.8 ± 0.1	0.5 ± 0.1	23 ± 1
Y224F§	8.2 ± 0.2 (16)	5.5 ± 0.1 (1.4)	3.4 ± 0.2 (7)	250 ± 7 (11)
Y224D§	40 ± 9 (80)	0.29 ± 0.03 (0.08)	24 ± 5 (48)	21 ± 2 (0.9)
Q222N§	15 ± 1 (30)	7.9 ± 0.3 (2)	5.0 ± 0.2 (10)	310 ± 5 (13)

† The values were determined in the presence of lithocholic acid at concentrations of 50 μ*M* for Y224D, 7 μ*M* for Q222N and 2 μ*M* for WT and Y224F. ‡ The values were determined in the presence of 5β-pregnane-3,20-dione at concentrations of 40 μ*M* for Y224D and 5 μ*M* for the other enzymes. § The values in parentheses are ratios of the mutant enzyme to the WT enzyme.

changes in the reduction of 17-ketosteroids than the other two mutants. Thus, the significant effects of replacing the bulky phenol ring of Tyr224 with an acidic side chain, together with the kinetic alterations arising from the Y224F and Q222N mutations, suggest that the orientation of the phenyl ring of Tyr224 is mediated by the hydrogen-bonding interaction between its hydroxyl group and the side chain of Gln222. Furthermore, the three mutations significantly increased the K_m values for NADP(H) (Table 3), confirming that Tyr224 plays a role in coenzyme binding through its interaction with Gln222.

The crystals of the Y224D mutant belonged to space group $P2_12_12$, which is the same space group in which the structure of apo WT AKR1C21 was solved previously (Faucher *et al.*, 2006), although the later was crystallized from different conditions (0.1 *M* MES pH 6.4, 0.2 *M* ammonium acetate and 16–18% PEG 4000). There were two monomers per asymmetric unit and electron density corresponding to the first three N-terminal residues and the coenzyme molecule was not observed in either monomer. In monomer *A*, electron density corresponding to residues 222–226 belonging to loop B was missing, probably as a consequence of structural disorder in this flexible region of the polypeptide chain. On the other hand, clear density was visible for residues 225 and 226 in monomer *B* (Fig. 3). Residues 3 and 4 in chain *A* and residues 3 and 223 in chain *B* were substituted by alanines in the model owing to a lack of electron density. Well defined electron densities were observed for all other main-chain and side-chain atoms of the polypeptide chain. A Ramachandran plot of backbone torsion angles for the refined structure showed that 92.9% of the residues were within favoured regions and 7.1% were in allowed regions. A summary of the data-collection and refinement statistics is presented in Table 4.

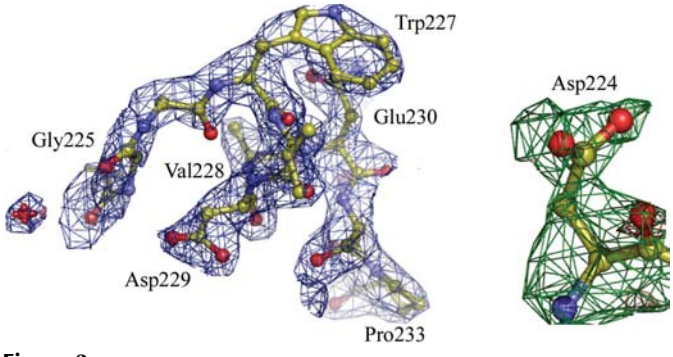

Figure 3
(*a*) $2F_o - F_c$ electron-density map corresponding to the refined model and contoured at a 1σ cutoff showing residues belonging to loop B. (*b*) Close-up view of the difference electron-density map ($F_o - F_c$) calculated after refinement of the model with Asp224 omitted and contoured at a 2σ cutoff.

Table 4
Summary of the data-collection and refinement statistics.

Values in parentheses are for the highest resolution shell.

Data collection and processing	
X-ray source	Rigaku RU300
Image plate	MAR 345
Wavelength (Å)	1.54179
Unit-cell parameters (Å, °)	a = 95.3, b = 97.8, c = 69.6, $\alpha = \beta = \gamma$ = 90
Space group	$P2_12_12$
Diffraction data	
Resolution range (Å)	30–2.3 (2.38–2.3)
Total No. of reflections	126514 (8729)
Unique reflections	28223 (2085)
Completeness (%)	98.8 (94.7)
Redundancy	4.3 (3.2)
$I/\sigma(I)$	13.3 (4.3)
R_{merge}†	5.5 (13.4)
Refinement (30–2.3 Å)	
R_{work}‡	0.174
R_{free}‡	0.276
Amino-acid residues	
Chain *A*	315
Chain *B*	321
Acetate ions	3
Water molecules	513
R.m.s. deviations	
Bond lengths (Å)	0.024
Angles (°)	2.1
Ramachandran plot	
Residues in favoured regions (%)	92.9
Residues in allowed regions (%)	7.1
Estimated coordinate error	
Luzzati plot (Å)	0.276
Average *B* factors (Å^2)	
Polypeptide chains *A* + *B*	28.25
Waters	34.6
Acetate ions	32.6

† $R_{merge} = \sum_{hkl}\sum_i |I_i(hkl) - \langle I(hkl)\rangle| / \sum_{hkl}\sum_i I_i(hkl)$, where $\langle I(hkl)\rangle$ is the average intensity over symmetry-related reflections and $I_i(hkl)$ is the observed intensity. ‡ $R = \sum_{hkl} ||F_{obs}| - |F_{calc}|| / \sum_{hkl} |F_{obs}|$, where F_o and F_c are the observed and calculated structure factors, respectively. For R_{free} the sum is performed on the test-set reflections (5% of total reflections) and for R_{work} on the remaining reflections.

The Y224D mutant enzyme consists of two identical polypeptide chains adopting a TIM-barrel motif in which the conformations of the catalytic residues Tyr55 and His117 are unaffected by the mutation. However, the conformation of loop B is strikingly different in the two molecules compared with the binary complex. AKR1C21 is one of the few AKRs for which the crystal structure has been determined both as an apoenzyme (in the absence of coenzyme) and as a holoenzyme (in the presence of coenzyme) (Faucher *et al.*, 2006; Dhagat *et al.*, 2007). In the crystal structure of the apoenzyme loop B has been reported to adopt an open conformation to allow coenzyme binding, following which it adopts a closed conformation. This conformational change brings the residues in loop B close to the active site, thereby locking the coenzyme in position and forming a mature substrate-binding site (Fig. 4). In the Y224D mutant enzyme loop B is in the open confor-

mation, in which the residues that would usually line the substrate-binding cavity in the WT holoenzyme are displaced away from the active site. The root-mean-square (r.m.s.) deviation between the C_α atoms of residues belonging to loop B in the Y224D mutant and the WT holoenzyme (PDB code 2p5n) was 2.61 Å. The orientation of loop B in the mutant enzyme is virtually identical to the conformation of loop B in the previously published structure of the apoenzyme (Faucher *et al.*, 2006). The r.m.s. deviation between the C^α atoms of these residues in the Y224D mutant and the WT apoenzyme (PDB code 2he8; Faucher *et al.*, 2006) was 0.76 Å.

Although the Y224D mutant enzyme was incubated with a threefold molar excess of the coenzyme NADPH during crystallization, in the refined crystal structure the active sites of both monomers lacked electron density for the coenzyme molecule. Instead, both monomers contained a water molecule and an acetate ion (from the crystallization buffer) that are involved in a hydrogen-bonding network with the catalytic residues (Fig. 5*a*). Most AKRs have a high affinity for the coenzyme molecule and AKR1C21 is one of the few AKRs for which the crystal structure has been solved in the absence of coenzyme. Nonetheless, the inability of the mutant enzyme to bind to the coenzyme molecule when it is present in excess during crystallization confirms the findings from the kinetic analysis, which showed that the Y224D mutation results in a 80-fold drop in the K_m for $NADP^+$ and a 48-fold drop in the K_m for NADPH (Table 3). In the mutant enzyme repulsion between the acidic side chain of aspartic acid and the pyrophosphate of the coenzyme would disfavour binding and causes loop B to remain in the open conformation.

In most AKRs the loop regions are quite flexible and their conformation is different in the presence and the absence of the coenzyme or substrate molecule. These conformational changes, which form a mature substrate-binding site, are responsible for proper substrate binding and product release (Hyndman *et al.*, 2003; Bennett *et al.*, 1996; Rees-Milton *et al.*, 1998). Upon comparison of the crystal structures of the WT binary and ternary complexes of AKR1C21 with the mutant enzyme, it is obvious that the mutation of Tyr224 to Asp224 affects the orientation of loop B, causing it to move further away from the active site and thereby changing the shape of the active-site cavity. The residues in loop B (Gly225 and Gly226) that interact with the substrates in the active site are no longer within hydrogen-bonding distance. Additionally, the formation of the unique V-shaped cavity formed by Tyr224 and Trp227 in the WT enzyme is no longer possible and the van der Waals contacts made by these residues with the substrates are lost (Fig. 5*b*). Mutation of the bulky phenol side

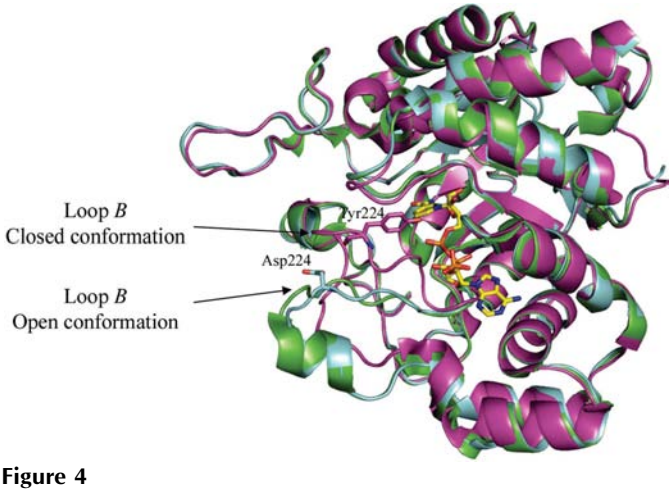

Figure 4
Superimposition of the WT holoenzyme (purple; PDB code 2p5n), WT apoenzyme (green; PDB code 2he8) and Y224D mutant (blue) structures. The TIM-barrel structure is unaffected by the mutation. The conformation of loop B in the WT holoenzyme (closed conformation) is different from that of the mutant and the apoenzyme, in which the loop adopts an open conformation, making the active site more accessible to allow coenzyme (yellow) binding.

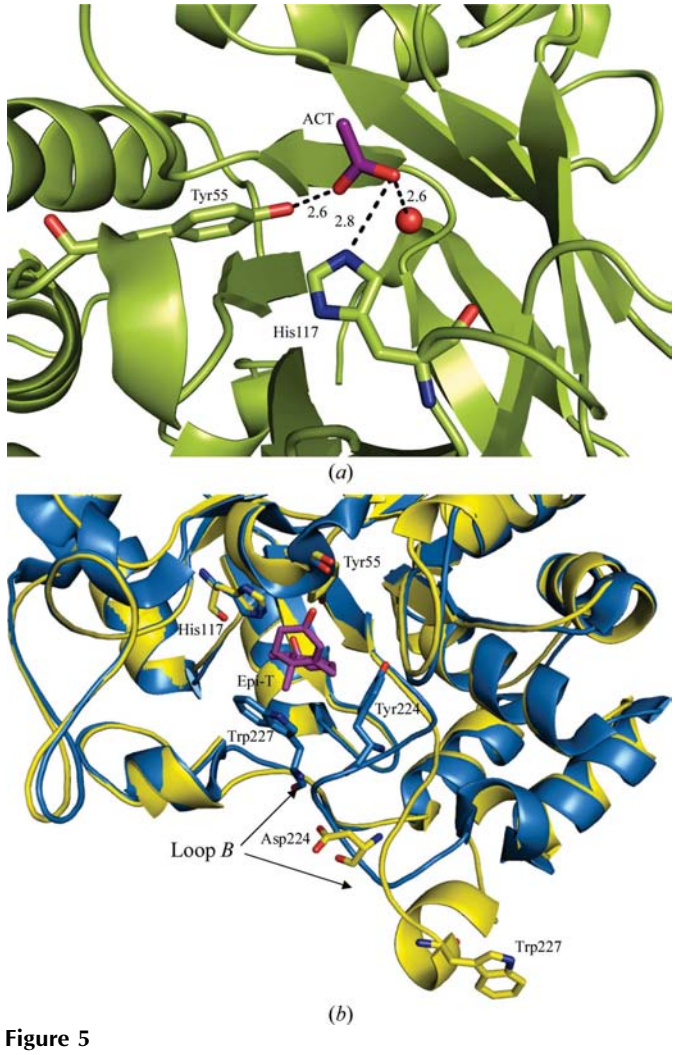

Figure 5
(*a*) The active site of the Y224D mutant enzyme is shown. In the absence of the coenzyme an acetate ion (ACT; purple) and a water molecule (red) are present within hydrogen-bonding distance of the catalytic residues Tyr55 and His117. Hydrogen bonds are shown as black dotted lines and the respective distances are marked in Å. (*b*) Superimposition of the WT epi-T-bound (PDB code 2ipf) and Y224D structures, showing the effect of mutation on the substrate-binding site. In the WT enzyme, Tyr224 together with Trp227 (blue) forms a V-shaped groove which positions the substrate in the active-site pocket. Owing to the mutation, loop B has moved away from the active site, in which residues Asp224 and Trp227 (yellow) no longer form van der Waals interactions with the modelled substrate.

chain to an acidic side chain reduces the affinity of the enzyme for the coenzyme and completely alters the stereospecificity of the enzyme, which exhibits 17β-HSD activity (Table 2). Overall, our study shows that the interaction between Tyr224 and other active-site residues such as Gln222 and Trp227 is critical as these interactions dictate the affinity of the enzyme for the coenzyme and its stereospecific oxidation of incoming 17α-hydroxysteroid substrates. Furthermore, our studies illustrate that the Y224D mutation disrupts the movement of the flexible loop B to the closed conformation, which holds the coenzyme in the binding site and positions incoming substrates for catalysis to occur.

References

Bellemare, V., Faucher, F., Breton, R. & Luu-The, V. (2005). *BMC Biochem.* **6**, 12.

Bennett, M. J., Schlegel, B. P., Jez, J. M., Penning, T. M. & Lewis, M. (1996). *Biochemistry*, **35**, 10702–10711.

Borhani, D. W., Harter, T. M. & Petrash, J. M. (1992). *J. Biol. Chem.* **267**, 24841–24847.

Collaborative Computational Project, Number 4 (1994). *Acta Cryst.* D**50**, 760–763.

Courter, L. A., Luch, A., Musafia-Jeknic, T., Arlt, V. M., Fischer, K., Bildfell, R., Pereira, C., Phillips, D. H., Poirier, M. C. & Baird, W. M. (2008). *Cancer Lett.* **265**, 135–147.

Dhagat, U., Carbone, V., Chung, R. P.-T., Schulze-Briese, C., Endo, S., Hara, A. & El-Kabbani, O. (2007). *Acta Cryst.* F**63**, 825–830.

Dhagat, U., Endo, S., Hara, A. & El-Kabbani, O. (2008). *Bioorg. Med. Chem.* **16**, 3245–3254.

Dhagat, U., Endo, S., Mamiya, H., Hara, A. & El-Kabbani, O. (2009). *Acta Cryst.* D**65**, 257–265.

Emsley, P. & Cowtan, K. (2004). *Acta Cryst.* D**60**, 2126–2132.

Faucher, F., Cantin, L., Pereira de Jesus-Tran, K., Lemieux, M., Luu-The, V., Labrie, F. & Breton, R. (2007). *J. Mol. Biol.* **369**, 525–540.

Faucher, F., Pereira de Jesus-Tran, K., Cantin, L., Luu-The, V., Labrie, F. & Breton, R. (2006). *J. Mol. Biol.* **364**, 747–763.

Hyndman, D., Bauman, D. R., Heredia, V. V. & Penning, T. M. (2003). *Chem. Biol. Interact.* **143–144**, 621–631.

Ishikura, S., Usami, N., Nakajima, S., Kameyama, A., Shiraishi, H., Carbone, V., El-Kabbani, O. & Hara, A. (2004). *Biol. Pharm. Bull.* **27**, 1939–1945.

Janecek, S. (1996). *Protein Sci.* **5**, 1136–1143.

Jez, J. M., Bennett, M. J., Schlegel, B. P., Lewis, M. & Penning, T. M. (1997). *Biochem. J.* **326**, 625–636.

Jez, J. M. & Penning, T. M. (2001). *Chem. Biol. Interact.* **130–132**, 499–525.

Jez, J. M., Schlegel, B. P. & Penning, T. M. (1996). *J. Biol. Chem.* **271**, 30190–30198.

Laskowski, R. A., Moss, D. S. & Thornton, J. M. (1993). *J. Mol. Biol.* **231**, 1049–1067.

Matsuura, K., Hara, A., Deyashiki, Y., Iwasa, H., Kume, T., Ishikura, S., Shiraishi, H. & Katagiri, Y. (1998). *Biochem. J.* **336**, 429–436.

Murshudov, G. N., Vagin, A. A. & Dodson, E. J. (1997). *Acta Cryst.* D**53**, 240–255.

Nakagawa, M., Tsukada, F., Nakayama, T., Matsuura, K., Hara, A. & Sawada, H. (1989). *J. Biochem. (Tokyo)*, **106**, 633–638.

Otwinowski, Z. & Minor, W. (1997). *Methods Enzymol.* **276**, 307–326.

Penning, T. M. (1999). *J. Steroid Biochem. Mol. Biol.* **69**, 211–225.

Penning, T. M., Jin, Y., Steckelbroeck, S., Lanisnik Rizner, T. & Lewis, M. (2004). *Mol. Cell. Endocrinol.* **215**, 63–72.

Penning, T. M., Pawlowski, J. E., Schlegel, B. P., Jez, J. M., Lin, H. K., Hoog, S. S., Bennett, M. J. & Lewis, M. (1996). *Steroids*, **61**, 508–523.

Rees-Milton, K. J., Jia, Z., Green, N. C., Bhatia, M., El-Kabbani, O. & Flynn, T. G. (1998). *Arch. Biochem. Biophys.* **355**, 137–144.

Storoni, L. C., McCoy, A. J. & Read, R. J. (2004). *Acta Cryst.* D**60**, 432–438.